Journal of The Electrochemical Society, 2021 **168** 031515
1945-7111/2021/168(3)/031515/8/$40.00 © 2021 The Electrochemical Society ("ECS"). Published on behalf of ECS by IOP Publishing Limited

Effect of Indium on the Negative Difference Effect for Magnesium Alloy

Tongyao Bao,[1,2] Lifeng Hou,[1,2,z] Junli Sun,[1,2] Xiaoda Liu,[1,2] Huayun Du,[1,2] Huan Wei,[1,2] and Yinghui Wei[1,2,z]

[1]*College of Materials Science and Engineering, Taiyuan University of Technology, Taiyuan 030024, Shanxi, People's Republic of China*
[2]*Corrosion and Protection Engineering Technology Research Center of Shanxi Province, Taiyuan, 030024, Shanxi, People's Republic of China*

The Mg-xIn (x = 0.5, 1, 1.5 wt.%) alloys exhibit the negative difference effect. This anomalous phenomenon was studied in 0.1 M NaCl solution using galvanostatic polarization testing and real-time hydrogen collection. Strong anomalous hydrogen evolution was observed in all three magnesium alloys, but the rate of hydrogen evolution at different anodic current densities decreased with the increased content of In element. It shows that adding indium to Mg can reduce the negative difference effect of Mg alloy. Assessment of the exchange current density for hydrogen evolution reaction supported the previously-proposed kinetic model. The exchange current density related to the hydrogen evolution reaction decrease with the increased content of In element, indicating the ability of magnesium alloys to support the cathodic reaction is weakened, and In element can effectively reduce the negative difference effect of magnesium alloy.
 [DOI: 10.1149/1945-7111/abee5c]

Manuscript submitted January 20, 2021; revised manuscript received March 6, 2021. Published March 22, 2021.

Magnesium (Mg) and its alloys, as the lightest metal structural materials, have received widespread attention. Very low density (1.74 g cm^{-3}) of magnesium makes it an attractive component for alloys, and because its metallurgy is simpler than that of other metals, it is also popular in the construction and the aircraft industries, and for optical and electronic devices.[1,2] Nevertheless, one of the main obstacles hindering the development and wider use of magnesium alloys is the poor corrosion resistance and complex dissolution behavior of Mg.[2–5] Hence, researching the basic principles of Mg and its alloys corrosion is the crucial step to improve the corrosion resistance and expand the application scope of Mg alloys. The overall Mg corrosion reaction is Eq. 1, and the cathodic and anodic half-reaction in neutral or alkaline media are Eqs. 2 and 3 respectively:[6]

$$Mg + 2H_2O \rightarrow Mg^{2+} + 2(OH^-) + H_2 \rightarrow Mg(OH)_2 + H_2 \quad [1]$$

$$2H_2O + 2e^- \rightarrow H_2 + 2OH^- \quad [2]$$

$$Mg \rightarrow Mg^{2+} + 2e^- \quad [3]$$

One molecule of hydrogen (H_2) is liberated for every atom of Mg that corrodes.[6] Therefore, measuring the volume of hydrogen gas (H_2) can directly obtain the corrosion of magnesium and its alloys.[7] The hydrogen evolution process of both pure magnesium and magnesium alloy has two characteristics: (1) the dominating cathodic process is hydrogen evolution reaction (HER). (2) The second characteristic is known as the negative difference effect (NDE).[6,8–10] The hydrogen evolution (HE) rate of magnesium and its alloys increases with increased of the polarization potential under the anodic polarization, which is also referred to as anomalous hydrogen evolution phenomenon. According to the well-accepted expression for activation-controlled kinetics theory,[2] the Butler-Volmer equation,[2] the rate of a cathodic reaction such as the HER should decrease exponentially and not increase with increasing anodic polarization potential.

In a word, the NDE always occurred in the corrosion process of magnesium and its alloys in the aqueous solution. There are many mechanisms that have been proposed to explain the NDE since it was first reported by Beetz,[11] there is still no consensus theory that can sufficiently explain the phenomenon of abnormal hydrogen evolution. The univalent Mg (Mg^+) theory is has been the most widely discussed theory, which is based on the assumption that the presence of Mg^+ is an intermediate in the anodic dissolution of Mg.[5,12–15] According to this mechanism, Mg metal dissolves to form univalent Mg^+ ions, and than Mg^+ ions are oxidised by water to produce hydrogen. More Mg^+ ions are produced as the rate of Mg dissolution increases under higher applied anodic potentials, thus increasing the rate of HE. Although this mechanism can explain the phenomenon of abnormal hydrogen evolution of magnesium and its alloys, no experimental technique has ever detected the presence of Mg^+. In addition, Swiatowska et al.[16] and Lebouil et al.[17] investigated the dissolution of Mg with atomic emission spectroelectrochemistry during potentiostatic control. The results of the study demonstrate that Mg dissolved as Mg^{2+} in chloride solution. In recent years, a kinetic model for the increase of HE rate with the increase of applied anode current densities were proposed by Frankel et al.[18–20] The kinetic model believes that high-activity hydrogen evolution surfaces will propose during the dissolution of magnesium, which has a stronger catalytic effect on HER, and increases with the increase of the anodic polarization time and the degree of anodic polarization.

Although the NDE has been extensively studied on the anodic polarization of pure magnesium, few studies on the behavior of magnesium alloys. So far, many scholars have studied the reprecipitation behavior of In and the influence of the addition of In on Al and Mg alloys.[21–24] The previous research studied the effects of the concentrations of In of magnesium alloys on microstructures and corrosion rate.[25] The study showed that the addition of In element could produce In and $In(OH)_3$, which fills the loose $Mg(OH)_2$ films to a certain extent. Gore et al. used particle induced X-ray emission spectroscopy and electrochemical techniques to investigate the influence of the noble alloying element enrichment on the cathodic activation of Mg-0.1 wt.% In and Mg-0.1 wt.% Au. [26] This research showed that magnesium indium alloy has higher anodically induced cathodic activation efficiency.[26] It is interesting and meaningful to investigate the influence of In element on the corrosion behavior of magnesium alloys. The purpose of this paper is to investigate the NDE of solid-solution Mg-In alloys subjected to anodic polarization in 0.1 M NaCl solution. And the kinetic model of the NDE, as mentioned above, was verified by solid-solution Mg-In alloys.

Materials and Methods

A high purity magnesium (Mg) (≥99.99%) ingot and high purity indium (In) (≥99.99%) ingot were used in this work. Magnesium-indium

[z]E-mail: houlifeng78@126.com; yhwei_tyut@126.com

alloys (Mg-xIn x = 0.5, 1, 1.5 wt.%) were melted with a medium frequency induction melting furnace under the protection of an inert atmosphere (Ar) in a graphite crucible. The indium (In) element has a high solid solubility in Mg, approximately 53.5 wt.% at 484 °C,[25,27–29] and the solubility is approximately 11 wt.% at room temperature.[30] The Mg-In alloy was solution treated at 450 °C for four hours in the resistance furnace and subsequently water quenched, which is conducive to the full diffusion of In in the Mg matrix and homogenization of the Mg-xIn alloys. The test specimens of solid solution Mg-xIn alloys were processed into a square shape of 12 mm × 12 mm × 8 mm. Samples were cold mounted in epoxy resin after a copper wire was attached to the rear part of the magnesium alloys and to expose the same working electrode surface area of about 1.44 cm^2. Next, a series of silicon carbide papers were used to grind the surface of samples to 2000 grit under anhydrous ethanol. Then, the samples were cleaned in an ultrasonic machine with the ethanol environment and dried with warmed air before the experiment.

Electrochemical testing was performed using a traditional three-electrode configuration. The working electrode was the solid-solution Mg-In alloy, the reference electrode was a saturated calomel electrode (SCE) and the counter electrode was a platinum mesh. The test equipment allowed collecting hydrogen during the simultaneous application of a galvanostatic signal. And a funnel and a burette filled electrolyte was used for hydrogen collection, described in detailed elsewhere.[16] The electrolyte solution was 0.1 M NaCl, and the pH is 6.4 in the initial phase. During electrochemical testing, to minimize the effects of ohmic potential drops, it was necessary to place the port of the luggin capillary as close as possible to the working electrode. The galvanostatic experiment was performed using different current densities in the range of −25 to +25 mA cm^{-2}, and hydrogen evolution was monitored by the volumetric method. We monitored the open circuit potential (OCP) of the samples for 15 min prior to the electrochemical testing to ensure a stable potential was reached.

The surface morphologies of solid solution Mg-xIn alloys after the galvanostatic experiment at different anodic current densities by scanning electron microscopy (SEM, TESCAN-VEGA3).

The cathodic potentiodynamic polarization curves prior to and following anodic galvanostatic experiment are compared to evaluate the catalytic properties of hydrogen evolution reaction (HER) on a pre-corroded surface of specimens. This approach was initially proposed by Birbilis et al.[20] The electrolyte needed to be replaced prior to the above experiment to avoid the effect of the value of pH change that has happened during the application of the galvanostatic treatment on the cathodic electrode kinetics.

Results and Discussion

The microstructure of solid-solution Mg-In alloys.—Figure 1 shows the microstructure, observed by the SEM, of Mg-0.5In, Mg-1In and Mg-1.5In alloy after solution treatment at 450 °C for 4 h. And Fig. 2 shows XRD patterns of the solid-solution Mg-xIn alloys. There is no secondary intermetallic in the microstructures and the XRD patterns. The Mg-In alloys have been solid solution treated, resulting in a large grain size. And the purpose of solid solution treatment is to eliminate the effect of second phase segregation.

Potentiodynamic polarization measurement of solid-solution Mg-In alloys.—Figure 3 plots the typical potentiodynamic polarization curves of solid-solution Mg-xIn (x = 0.5, 1, 1.5 wt.%) alloys at room temperature in 0.1 M NaCl solution, and the potentiodynamic polarization curve of the high purity magnesium (HP Mg) is also shown for comparative purposes. The experiment was repeated three times, and with good reproducibility. The electrode potential was scanned from −500 mV vs E_{corr} to 500 mV vs E_{corr}, and the scan rate was 1 mV s^{-1}. It can be observed that there are significant differences between HP Mg and solid-solution Mg-xIn alloys. The HP Mg has an E_{corr} about −1.62 V_{SCE} with no evidence of passivity and no sign of pitting, while the solid-solution Mg-In alloys have E_{corr} values that are significantly lower than HP Mg. The corrosion potential of Mg-0.5In, Mg-1In and Mg-1.5In is −1.85 V_{SCE}, −1.88 V_{SCE} and −1.88 V_{SCE}, respectively, suggesting that the addition of In element will decrease the corrosion potential of magnesium alloy. And all of the Mg-xIn samples have a slight passivation region indicating that a protective film has formed on the surface. An

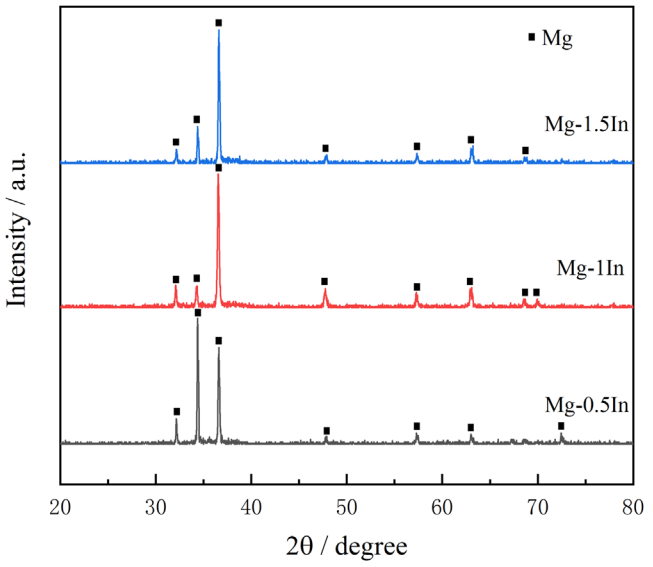

Figure 2. XRD patterns of the solid-solution Mg-0.5In, Mg-1In and Mg-1.5In alloy.

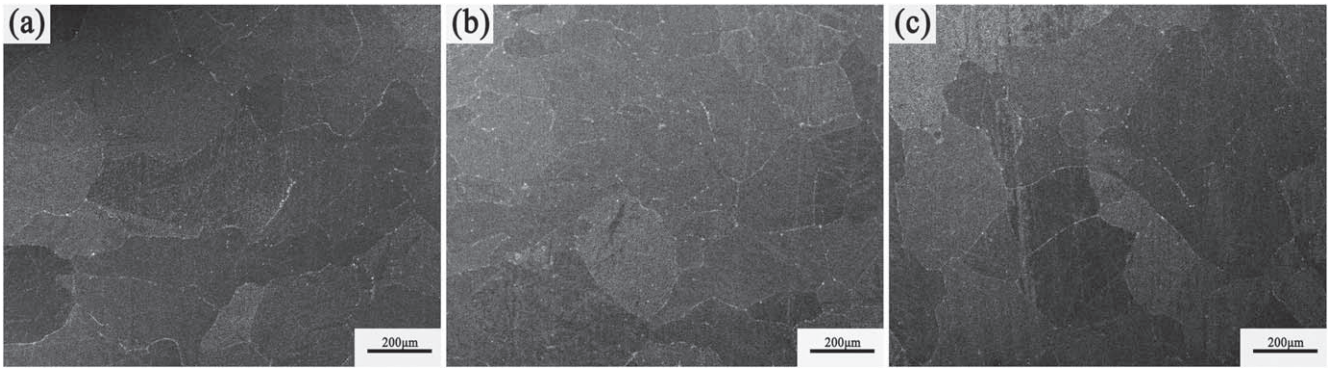

Figure 1. Microstructure of Mg-In alloys after solution treatment at 450 °C for 4 h. (a) solid-solution Mg-0.5In alloy, (b) solid-solution Mg-1In alloy and (c) solid-solution Mg-1.5In alloy.

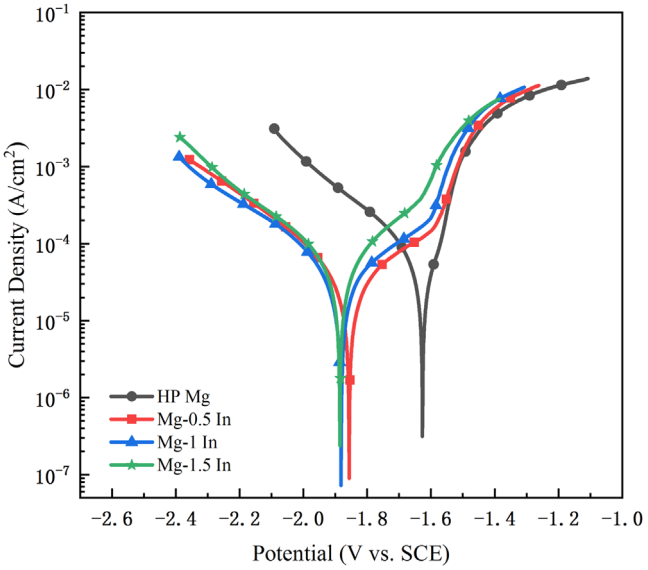

Figure 3. Typical potentiodynamic polarization curves of the solid-solution Mg-0.5In, Mg-1In and Mg-1.5In alloy in 0.1 M NaCl solution.

increase in passivity suggests a decrease in NDE. Compared with HP Mg, the current density of cathodic branch is lower for three kinds of solid-solution Mg-In alloys, suggesting that the corrosion is inhibited and the cathodic kinetics reduced by the addition of indium into the magnesium matrix. Note that even though the cathodic kinetics are reduced, the anodic kinetics are enhanced slightly.

Hydrogen evolution collection during anodic galvanostatic polarization.—Figures 4 and 5 shows the volume of hydrogen gas (H_2) collected during galvanostatic polarization tests, application of different anodic and cathodic current densities, as a function of time in 0.1 M NaCl solution for the solid-solution Mg-In alloy electrodes. These two figures show the typical results of three repeated tests, and the error bars are drawn. As can be seen from Figs. 4 and 5, in all cases, the function relation between HE quantity and time is relatively linear. The volume of hydrogen evolution of three kinds of Mg-xIn alloys increases with increaseing applied anodic current density, which is evidence of the NDE. It can be observed that volume of H_2 decreases with the rise of the content of In element within the whole range of applied anodic current densities. The volume of H_2 of Mg-0.5In alloy is 5 ml cm^{-2} and 13 ml cm^{-2} at the highest applied anodic and cathodic current density (i.e., 25 mA cm^{-2}), respectively, which are much higher than the Mg-1In and Mg-1.5In. This phenomenon may be due to the surface film formed by Mg-0.5In at the highest current density cannot protect the magnesium alloy substrate. When the cathodic current density is applied, with the increase of In content, the amount of hydrogen evolution slightly decreases. However, the amount of hydrogen evolution of the three alloys is not much different, which should be the case since the HE rate ought to depend only on the applied cathodic current density.

H_2 is very soluble in an aqueous solution, so some H_2 was dissolved at the beginning of the experiment, and some H_2 would accumulate on the walls of the glass funnel and burette. So the amount of HE obtained in the galvanostatic experiment was less than

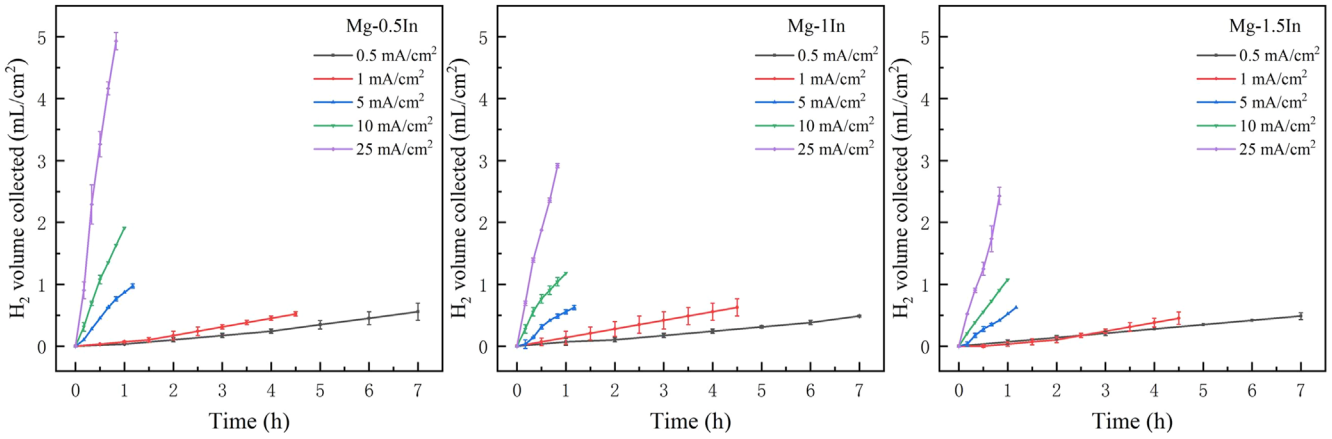

Figure 4. Volume of hydrogen, collected at the different applied anodic current densities, as a function of time for the solid-solution Mg-0.5In, Mg-1In and Mg-1.5In alloy in 0.1 M NaCl solution.

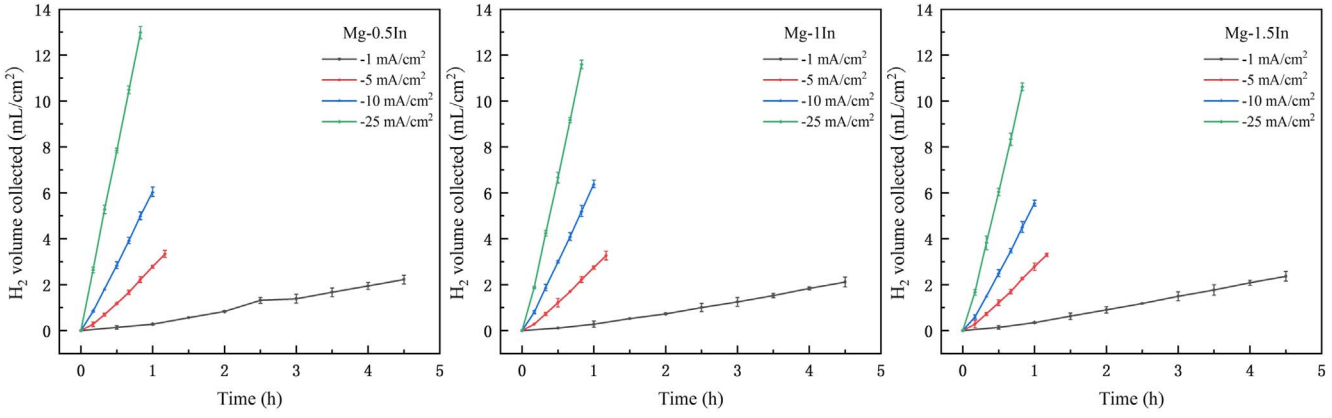

Figure 5. Volume of hydrogen, collected at the different applied cathodic current densities, as a function of time for the solid-solution Mg-0.5In, Mg-1In and Mg-1.5In alloy in 0.1 M NaCl solution.

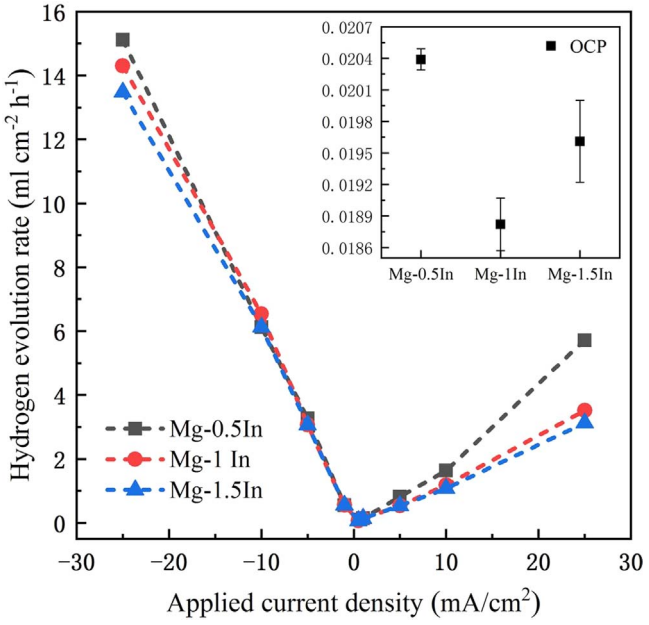

Figure 6. The rate of HE on the solid-solution Mg-0.5In, Mg-1In and Mg-1.5In alloy as a function of the applied anodic current densities in 0.1 M NaCl solution. The rate of HE of the solid-solution Mg-0.5In, Mg-1In and Mg-1.5In alloy at OCP.

that actually produced. The HE rates of solid-solution Mg-In alloys as a function of the applied current densities figures are plotted in Fig. 6. And the HE rates of solid-solution Mg-In alloys at OCP are shown in Fig. 6. We have done many duplicate experiments, and the typical results are drawn. The behavior is very similar to that previously reported for high purity magnesium by Fajardo et al.[19] The HE rates increased with increasing applied anodic and cathodic current densities and reached a minimum at the OCP. This is expected in Cl^- containing solution.[3] In the whole applied anodic current density range, the comparison shows that the HE rate of Mg-0.5In alloy is the highest, followed by Mg-1In and Mg-1.5In. The HE rate was rather high for Mg-0.5In alloy, approximately 1.8 times of Mg-1.5In at the highest anodic current density. The HE rate of the solid solution Mg-In alloy decreased with the increase of content of the In element at applied anodic current densities. The HE rate of a solid solution Mg-0.1In alloy has been measured by Gore et al.[26] An HE rate of a solid solution Mg-0.1In alloy are 2.5 ml cm^{-2} h^{-1} at 5 mA cm^{-2} and 4 ml cm^{-2} h^{-1} at 10 mA cm^{-2} for this alloy which provides additional data points to support the trend. The effect of the

Table I. Calculated the effect of the NDE of the solid-solution Mg-0.5In, Mg-1In and Mg-1.5In alloy at different applied anodic current densities in 0.1 M NaCl solution.

	The effect of the NDE		
Applied current density (mA cm^{-2})	Mg-0.5In	Mg-1In	Mg-1.5In
0.5	−0.084	−0.051	−0.050
1	−0.119	−0.120	−0.119
5	−0.797	−0.515	−0.514
10	−1.614	−1.162	−1.057
25	−5.699	−3.495	−3.108

NDE can be calculated by Eq. 4:

$$\Delta K = K_0 - K_1 \quad [4]$$

where ΔK is the effect of the NDE, K_0 is the HE rates without any applied current density, K_1 is the rate of HE at the applied anode current density. Table I shows the effect of the NDE, calculated by Eq. 4, of the solid-solution Mg-0.5In, Mg-1In and Mg-1.5In alloy at different applied anodic current densities in 0.1 M NaCl solution. Therefore, these phenomena indicate the highest NDE of the Mg-0.5In alloy studied and the relatively lowest NDE of the Mg-1.5In alloy. The results from the solid-solution Mg-xIn (x = 0.5, 1, 1.5 wt.%) alloys are very similar in the whole range of cathodic current densities.

The rate of HE can be converted to a current density for the HE using Faraday's law:

$$i_{H_2} = \frac{PVFj}{RTSt} = \frac{PFj}{RT} \cdot \frac{V}{St} \quad [5]$$

where (i_{H_2}) is the current density for the HE, P is the atmospheric pressure, F is the Faraday constant, j is the valence involved in the electrode reaction, R is the ideal gas constant, T is the thermodynamic temperature during this testing, V is the volume of H_2 collected, S is the superficial area of working electrode, t is the time of galvanostatic polarization. Figure 7 plots the current densities for the HE (i_{H_2}) calculated by Eq. 5 while applying different anodic and cathodic current densities as a function of the potential. The representative results of duplicate experiments are plotted. However, HER took place at the full range of anodic and cathodic galvanostatic polarization, with the applied current density increases, abundant hydrogen bubbles produced at the surface of the working electrode, resulting in larger resistances. Moreover, it is difficult to measure ohmic potential drop by the current interrupt method (CI) because of the excessive amount of hydrogen bubbles. Therefore, the

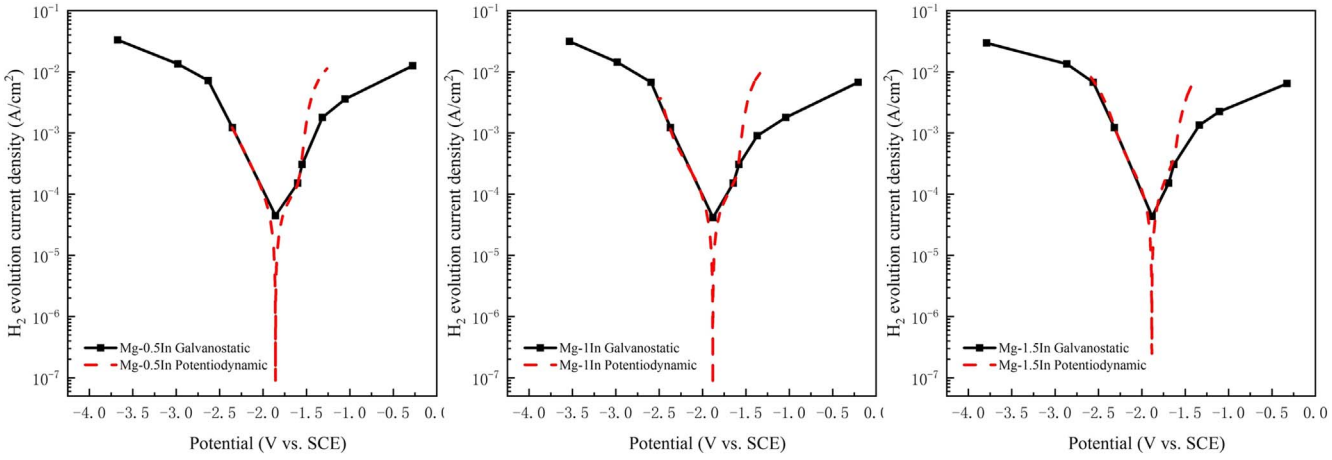

Figure 7. Current density of the HE calculated by Eq. 5 for the solid-solution Mg-0.5In, Mg-1In and Mg-1.5In alloys as a function of the potential, and we need note that the measured potentials are not corrected for the ohmic potential drop.

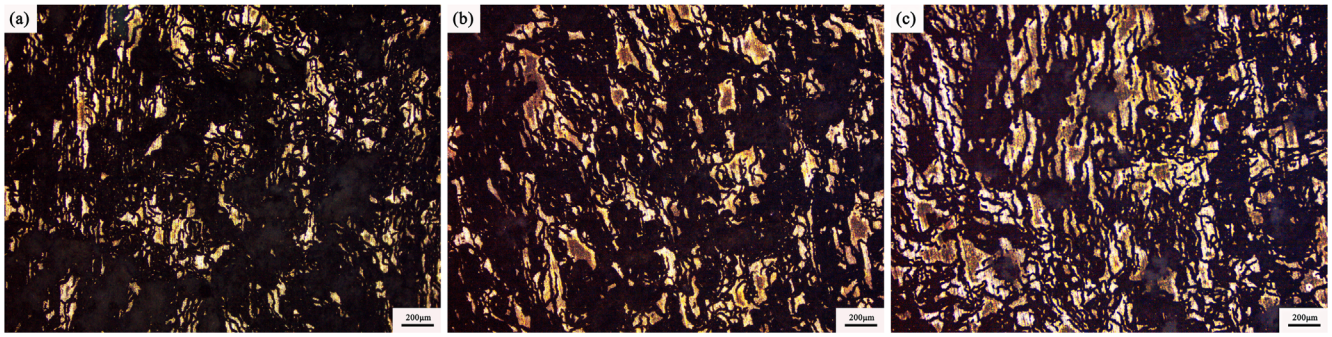

Figure 8. The optical micrographs of the surface appearance of the (a) Mg-0.5In, (b) Mg-1In, (c) Mg-1.5In alloy after the application of anodic current densities about 10 mA cm^{-2} in 0.1 M NaCl solution.

data in Fig. 7 have not been corrected for the ohmic potential drop. The potentiodynamic polarization curves of solid-solution Mg-xIn alloys taken from Fig. 3 are also drawn with dashed lines for comparative purposes. It can be seen that the correlation is excellent, especially in the regions close to OCP, the good correlation on the cathodic side would be justification of the method. It is worth noting that the current densities at potentials above the OCP (i.e., the range over the whole anodic) were calculated from the HE data reported for the galvanostatic experiments. When an anodic current is applied galvanostatically, a net anodic current of a certain value flows through the electrochemical cell in addition to the corresponding corrosion current density.

The metallography images illustrating the macroscopic appearances of the solid-solution Mg-xIn alloys after the galvanostatic polarization tests at the application of anodic current density about 10 mA cm^{-2} are plotted in Fig. 8. The macroscopic morphology at this current density is typical. All the Mg-In alloys exhibited a surface covered with filiform tracks, which confirms that dissolution during anodic polarisation is not uniform as reported by Birbilis et al.[20] As the content of In element increased, the coverage of the filiform corrosion product decreased gradually, indicating that the In element affected the corrosion resistance for the magnesium alloy.

Figure 9 shows the microtopography, observed by the SEM, of the solid-solution Mg-0.5In, Mg-1In and Mg-1.5In alloy, respectively, after different applied anodic current densities in 0.1 M NaCl solution. It can be observed that the corrosion products have accumulated on the surface of the working electrodes, and cracks have appeared on the surface of alloys, indicating that different degrees of corrosion has occurred on the surface. The degree of the corrosion product increased with increasing applied anodic current densities. Observation of the corrosion morphology indicated that fewer cracks at lower applied anodic current densities (i.e., Figs. 9a–9f) appeared. Furthermore, the extent of corrosion increased at higher current densities (i.e., Figs. 9g–9o). The comparison of the corrosion morphology of the solid-solution Mg-xIn alloys at different applied anodic current densities shows that the surface cracks of the Mg-In alloy in 0.1 M NaCl solution under the same anodic current densities are reduced with the increase of In content, the corrosion is inhibited and the corrosion resistance of the alloy is improved in the order of Mg-0.5In < Mg-1In < Mg-1.5In.

Cathodic potentiodynamic polarization testing on corroded solid-solution Mg-In alloy surface.—Figure 10 shows the cathodic potentiodynamic polarization curves measured in 0.1 M NaCl solution for solid-solution Mg-xIn alloys following treatment at different anodic current densities (i.e., 0.5, 1, 5, 10, 25 mA cm^{-2}). These figures show the typical results of three duplicate experiments. The cathodic potentiodynamic polarization response of the working electrode without prior galvanostatic experiments are also shown in the Fig. 10 for comparative purposes. The increases of cathodic current densities were observed after galvanostatic anodic current density was applied, implying cathodic kinetics (i.e., the kinetics of the HER) are significantly higher and enhancement of the ability to support the cathodic reaction rate. The cathodic polarization curve of the solid-solution Mg-xIn alloys after anodic galvanostatic polarization at a lower current density (i.e., 0.5 mA cm^{-2}) exhibit the largest increase compared to the specimens unsubjected to polarization. That indicates a significant increase in catalytic activity for HER on the surface of Mg-In alloys when the lowest anodic current density was applied. However, Fig. 9 shows that the amount of corrosion products of Mg-In alloys surfaces increases with the applied current density, so suggests that the corrosion products film is not a dominating component in the enhancement of the HER. Besides, no significant difference was observed in the cathodic potential response between the three Mg-In alloys previously undergoing anodic galvanostatic polarization. This is inconsistent with the concept of anomalous HE caused by corrosion products. The corrosion potential (E_{corr}) of the Mg-In alloys shifts towards more positive potential on corroded surfaces. That was likely due to decrease in the anodic kinetics, resulting in a net cathodic current appeared in the region that was previously dominated by the anodic dissolution reaction of the Mg-In alloys.[31,32] It is evident that the formation of a corrosion product film (see Fig. 9) may have partially protected the surface decreasing the anodic kinetics.

Influence of hydrogen evolution kinetics.—Assuming that the electrochemical corrosion of magnesium alloys follows activation controlled kinetics, the Butler-Volmer equation shown in Eq. 6 describing HER can be simplified to the Tafel Eq. 7[2,19] when the electrode potential (E) is much higher than the reversible potential ($E_{rev,H}$):

$$i_{\mathrm{HER}} = i_{0,H,\mathrm{Mg}}\left[\exp\left(\frac{(E - E_{rev,H})}{b_a}\right) - \exp\left(\frac{-(E - E_{rev,H})}{|b_c|}\right)\right] \quad [6]$$

$$i_{\mathrm{HER}} = i_{0,H,\mathrm{Mg}}\exp\left(\frac{-(E - E_{rev,H})}{|b_c|}\right) \quad [7]$$

where i_{HER} is the current density of HER, $i_{0,H,Mg}$ is the exchange current density of the hydrogen evolution on Mg-In alloy, $|b_c|$ is the absolute value of the cathodic Tafel slope. If the $E_{rev,H}$, $i_{0,H,Mg}$ and $|b_c|$ are fixed, the rate of HER should decrease exponentially as E increases according to Eq. 7. However, the HER rate in fact increases as E increases in the anodic region of polarization, as the unique phenomenon we observed. Therefore, this anomalous phenomenon may be caused by the change of other parameter values in Eq. 7.

According to the Nernst equation of hydrogen evolution reaction:[18]

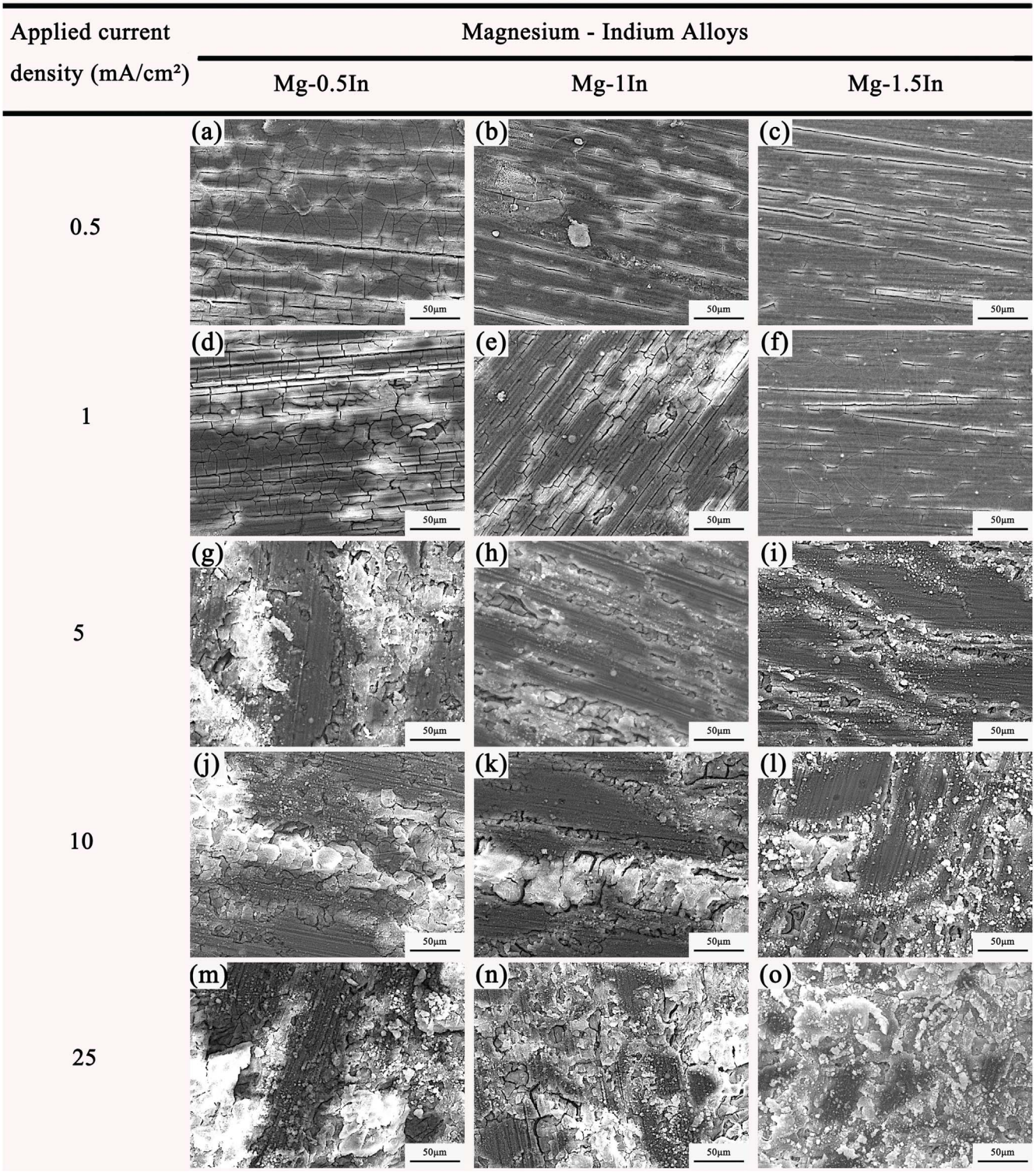

Figure 9. The microtopography, observed by the SEM, of the solid-solution Mg-xIn working electrodes after different applied anodic current densities in 0.1 M NaCl solution.

$$E_{\mathrm{rev},H} = -0.00591\, pH \qquad [8]$$

$E_{rev,H}$ only depends on the pH value of the solution and not directly on the electrode properties. Besides, b_c is the cathodic Tafel slope, which can be regarded as a fixed value. As a result, the high rates of HE in the anodic region might be caused by the change of $i_{0,H,Mg}$.[18]

The value of exchange current density for HER of magnesium alloy with different anode current densities can be obtained by extrapolating the cathode Tafel line to the equilibrium potential for HER ($E_{rev,\ H}$).[19] Assuming that the pH of electrolyte solution before the galvanostatic polarization experiment is 7 for comparison, and then $E_{rev,H} = -0.653\ \mathrm{V_{SCE}}$.

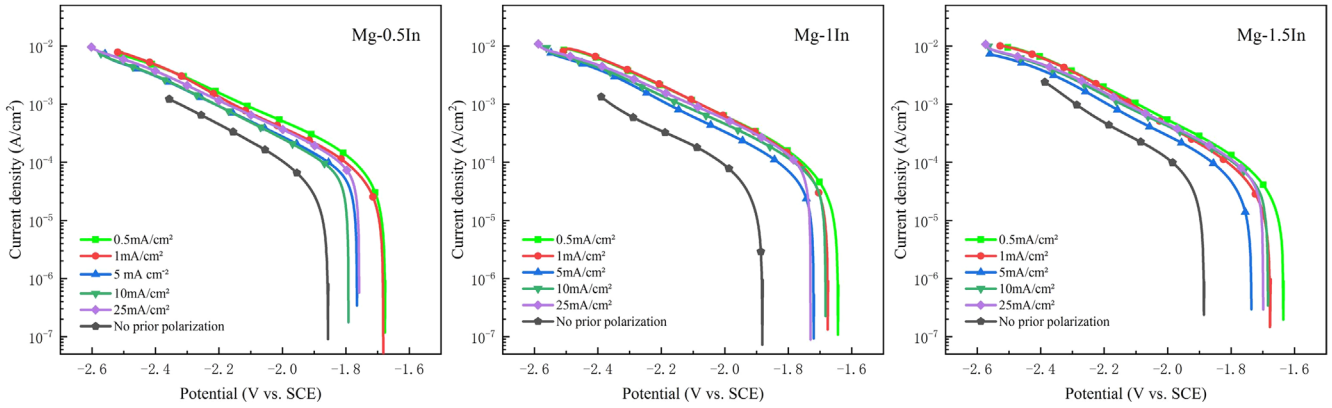

Figure 10. Cathodic potentiodynamic polarization curves for the solid-solution Mg-0.5In, Mg-1In and Mg-1.5In alloy after galvanostatic polarization testing at different applied anodic current densities. The potentiodynamic polarization curves of the solid-solution Mg-In alloys without prior galvanostatic polarization are also plotted in this figure.

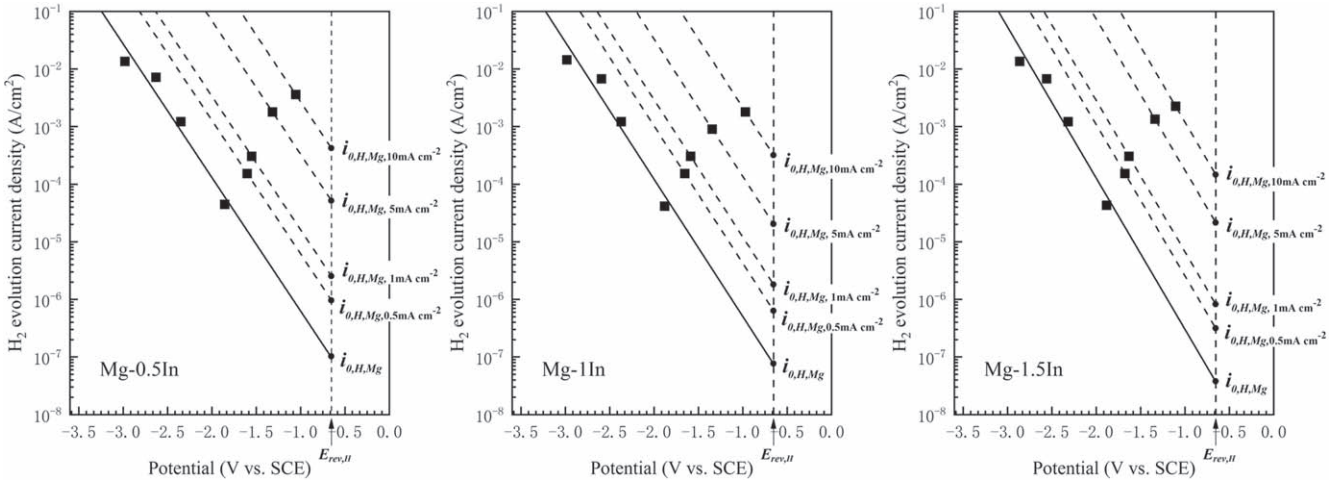

Figure 11. The extrapolations of the Tafel slopes fitted by the cathodic region to a potential of $-0.653\ V_{SCE}$. And the extrapolations results overlay onto data taken from Fig. 5 to calculate the HER exchange current density for solid-solution Mg-0.5In, Mg-1In and Mg-1.5In alloy at the different application of anodic current densities.

Figure 11 shows the extrapolations of the Tafel slopes fitted by the cathodic region to a potential of $-0.653\ V_{SCE}$, the data points in this figure are within the potential range close to OCP in Fig. 5, because the ohmic potential drops are minimised. The Tafel slopes of the solid-solution Mg-xIn alloys were obtained from the linear fit of the cathodic Tafel lines, resulting the Tafel slopes (i.e., the values of b_c) are $-0.43\ V\ dec^{-1}$, $-0.42\ V\ dec^{-1}$ and $-0.39\ V\ dec^{-1}$, respectively. Indicating that the Tafel slope of solid-solution Mg-xIn alloys decreased gradually with the increase of In element, but the difference is smaller.

Figure 11 provides the value of $i_{0,H,Mg}$ in the cathodic part of the curve of solid-solution Mg-xIn alloys are about 1.0×10^{-7}, 7.7×10^{-8}, and $3.8 \times 10^{-8}\ A\ cm^{-2}$ respectively. It can be observed that the value of $i_{0,H,Mg}$ for the cathodic region gradually decreases with the increase concentration of In element. Where Mg-0.5In is relatively compared with the Mg-1.5In, the $i_{0,H,Mg}$ of the cathodic region increased by about 2.6 times. Confirming that a lower catalytic ability for the alloys surface with a higher concentration of In element. It is worth noting that the difference of the value of $i_{0,H,Mg}$ at the cathodic region for the three kinds of Mg-xIn alloys is not very much, which may be due to the small difference in the content of In in the Mg-xIn alloys in this experiment. The three magnesium alloys all exhibited an increase in the exchange current density for HER with increasing prior anodic current density applied, which indicates a large increase in the catalytic activity of the dissolving Mg-In alloys surface. This result confirmed the model for improving anodic HE based on increasing exchange current density proposed by Frankel et al.[18,19] The increase of hydrogen evolution rate is due to the increase of exchange current density for HER. Table II shows the values of exchange current density for HER obtained by the above method for the solid-solution Mg-In alloys after the different applied anodic current densities in 0.1 M NaCl solution. The exchange current density of the magnesium alloy in the cathodic part ($i_{0,H,Mg}$) is reduced by 1–2 orders compared with pure magnesium (i.e., $i_{0,H,Mg} = 4 \times 10^{-6}\ A\ cm^{-2}$) reported by Frankel et al.[18] The addition of In can reduce the exchange current density of the magnesium alloy, and it is reasonable that the catalytic properties of these surfaces towards the HER (namely the exchange current density) may vary with the amount of this alloying element. The exchange current density for HER showed an enormous increase in all the samples after the applied different anodic current densities. The increment reached approximately orders of magnitude at the higher applied anodic current density (i.e., $10\ mA\ cm^{-2}$) for the solid-solution Mg-0.5In, Mg-1In and Mg-1.5In alloy, exhibiting a considerable enhancement in the hydrogen evolution kinetics, and the results are consistent with Fig. 10. However, the degree of enhancement is much lower than that of both pure magnesium and high pure magnesium reported by Fajardo et al.,[19] indicating that the addition of In element can reduce the HE kinetics and the surface catalytic activity of the magnesium. In addition, the increment of the

Table II. The exchange current density for HER of the Mg-0.5In, Mg-1In and Mg-1.5In alloy at the different applied current densities.

Applied current density (mA cm^{-2})	Exchange current density for HER (A cm^{-2})		
	Mg-0.5In	Mg-1In	Mg-1.5In
OCP	1.0×10^{-7}	7.7×10^{-8}	3.8×10^{-8}
0.5	9.7×10^{-7}	6.3×10^{-7}	3.1×10^{-7}
1	2.5×10^{-6}	1.8×10^{-6}	8.3×10^{-7}
5	5.2×10^{-5}	2.1×10^{-5}	2.0×10^{-5}
10	4.2×10^{-4}	3.2×10^{-4}	1.5×10^{-4}

exchange current density for HER decreased gradually as the increased content of In element.

Conclusions

The anomalous HE on solid-solution Mg-xIn (x = 0.5, 1, 1.5 wt.%) alloys was investigated using galvanostatic polarization measurements coupled with H_2 collection. The following can be concluded:

1. Anomalous HE was observed on the three kinds of solid-solution Mg-xIn (x = 0.5, 1, 1.5 wt.%) alloys during the different anodic galvanostatic applied.
2. Adding indium to magnesium can reduce the negative difference effect. The rate of HE measured under anodic galvanostatic polarization showed a clear dependence on the concentration of In in the Mg alloy. The anomalous rate of HE decreases with increases In content.
3. As the content of In element increased, the coverage of the corrosion product decreased gradually. Besides, no significant difference was observed in the cathodic potential response between the three Mg-In alloys previously undergoing anodic galvanostatic polarization. This is inconsistent with the concept of anomalous HE caused by corrosion products.
4. The NDE of Mg-In alloys results from the enhancement in the catalytic activity for HER on dissolving alloys surfaces. The enhancement of catalytic activity was quantified by the exchange current density ($i_{0,H,Mg}$) of hydrogen evolution reaction during anodic polarization. The rate of HE for the solid-solution Mg-xIn (x = 0.5, 1, 1.5 wt.%) alloys increases with the increase of exchange current densities of HE. This supports the prediction of the kinetic model proposed previously.

Acknowledgments

This work was supported by the National Natural Science Foundation of China (No. 52071227), Key Scientific Research Project in Shanxi Province (Grant No. 201805D121003), Special Found Projects for Central Government Guidance to Local Science and Technology Development, Science and Technology Major Projects of Shanxi Province (20191102004), Natural Science Foundation of Shanxi Province of China (2019D111102), Research Project Supported by Shanxi Scholarship Council of China (HGKY2019085).

ORCID

Yinghui Wei https://orcid.org/0000-0002-8420-681X

References

1. P. Knochel, *Nat. Chem.*, **1**, 740 (2009).
2. M. Esmaily, J. E. Svensson, S. Fajardo, N. Birbilis, G. S. Frankel, S. Virtanen, R. Arrabal, S. Thomas, and L. G. Johansson, *Prog. Mater Sci.*, **89**, 92 (2017).
3. T. W. Cain, I. Gonzalez-Afanador, N. Birbilis, and J. R. Scully, *J. Electrochem. Soc.*, **164**, C300 (2017).
4. G. Song, B. Johannesson, S. Hapugoda, and D. StJohn, *Corros. Sci.*, **46**, 955 (2004).
5. G. Song and A. Atrens, *Adv. Eng. Mater.*, **5**, 837 (2003).
6. A. Atrens, G.-L. Song, M. Liu, Z. Shi, F. Cao, and M. S. Dargusch, *Adv. Eng. Mater.*, **17**, 400 (2015).
7. G. L. Song, A. Atrens, and D. John St, *Magnes. Technol.*, 255 (2001).
8. A. Atrens, M. Liu, N. I. Z. Abidin, and G. L. Song, *Corrosion of Magnesium Alloys*, 117 (2011).
9. A. Atrens, G.-L. Song, F. Cao, Z. Shi, and P. K. Bowen, *Journal of Magnesium and Alloys*, **1**, 177 (2013).
10. S. Lebouil, O. Gharbi, P. Volovitch, and K. Ogle, *Corrosion*, **71**, 234 (2015).
11. W. Beetz, *The London, Edinburgh, and Dublin Philosophical Magazine and Journal of Science*, **32**, 269 (2009).
12. R. L. Petty, A. W. Davidson, and J. Kleinberg, *J. Am. Chem. Soc.*, **76**, 363 (1954).
13. G. L. Song and A. Atrens, *Adv. Eng. Mater.*, **1**, 11 (1999).
14. A. Atrens, M. Liu, and N. I. Z. Abidin, *Materials Science and Engineering: B,*, **176**, 1609 (2011).
15. Z. Shi, J. X. Jia, and A. J. C. S. Atrens, *Corros. Sci.*, **60**, 296 (2012).
16. J. Światowska, P. Volovitch, and K. Ogle, *Corros. Sci.*, **52**, 2372 (2010).
17. S. Lebouil, A. Duboin, F. Monti, P. Tabeling, P. Volovitch, and K. Ogle, *Electrochim. Acta*, **124**, 176 (2014).
18. G. S. Frankel, A. Samaniego, and N. Birbilis, *Corros. Sci.*, **70**, 104 (2013).
19. S. Fajardo and G. S. Frankel, *Electrochim. Acta*, **165**, 255 (2015).
20. N. Birbilis, A. D. King, S. Thomas, G. S. Frankel, and J. R. Scully, *Electrochim. Acta*, **132**, 277 (2014).
21. M. C. Reboul, P. Gimenez, and J. J. Rameau, *Corrosion*, **40**, 366 (1984).
22. A. G. Muñoz, S. B. Saidman, and J. B. Bessone, *Corros. Sci.*, **44**, 2171 (2002).
23. J. Li, B. Zhang, Q. Wei, N. Wang, and B. Hou, *Electrochim. Acta*, **238**, 156 (2017).
24. P. Gore, S. Fajardo, N. Birbilis, G. S. Frankel, and V. S. Raja, *Electrochim. Acta*, **293**, 199 (2019).
25. M. Yin, L. Hou, X. Liu, Z. Wang, B. Liu, J. Jia, S. Zhang, and Y. Wei, *J. Alloys Compd.*, **811** (2019).
26. P. Gore, T. Cain, J. Laird, J. Scully, N. Birbilis, and V. Raja, *Corros. Sci.*, **151**, 206 (2019).
27. J. Li, K. Wan, Q. Jiang, H. Sun, Y. Li, B. Hou, L. Zhu, and M. J. M. Liu, *Metals*, **6**, 65 (2016).
28. Y. Dong, B. Z. Sun, J. Tan, Y. H. Sun, and X. D. Sun, *Mater. Lett.*, **277**, 128367 (2020).
29. P. Feschotte, *Journal of The Less-Common Metals*, **46**, 51 (1976).
30. C. Zhou, Z. Z. Fang, J. Lu, and X. Zhang, *J. Am. Chem. Soc.*, **135**, 10982 (2013).
31. G. Williams, N. Birbilis, and H. N. J. E. C. Mcmurray, *Electrochem. Commun*, **36**, 1 (2013).
32. S. Fajardo, C. F. Glover, G. Williams, and G. S. Frankel, *Electrochim. Acta*, **212**, 510 (2016).